

## **VIII- II -1. Project Research**

### **Project 4**

Y. Kawabata

*Research Reactor Institute, Kyoto University*

### OBJECTIVES AND ALLOTTED RESEARCH SUBJECTS :

The aim of this project research is the development on neutron imaging and its application.

ARS-1 Development on neutron imaging application in KUR

ARS-2 Measurements of multiphase dynamics by neutron radiography

ARS-3 Visualization of two-phase flow in a polymer electrolyte fuel cell

ARS-4 Neutron radiography on tubular flow reactor for supercritical hydrothermal synthesis of nanoparticles

ARS-5 Characteristics of the void fraction under a forced convective flow boiling

ARS-6 Relationship between plant root system and water movement in rice hull medium

ARS-7 Neutron imaging of industrial components and simulation using VCAD system

ARS-8 Measurement of water content in hardened cement paste by neutron imaging

ARS-9 In-situ measurement of the hydraulic behavior of high strength concrete under high temperature

ARS-10 Hydrazine decomposition phenomena observed by neutron radiography at a catalyst bed

ARS-11 Development of neutron imaging devices

### MAIN RESULTS AND THE CONTENTS OF THIS REPORT :

Y. Kawabata et al. (ARS-1) did not perform their experiments in KUR.

Y. Saito et al. (ARS-2) applied a spatio-temporal filter to high frame-rate neutron radiography to enhance quality of images and to compare the effect of neutron flux from the neutron sources. The proposed one has been applied to images obtained at the B4-port of KUR and at the JRR-3 of JAEA. The results show that the severe signal noises could be removed from the original images by applying the modified bilateral filter, while preserving the edge information.

N. Takenaka et al. (ARS-3) have measured the water behavior in a polymer electrolyte fuel cell (PEFC) by using neutron radiography for understanding the water

distributions in the PEFC with and without micro porous layer (MPL) and show that the MPL makes change the distribution of water condensation rate in the gas diffusion layer (GDL).

T. Tsukada et al. (ARS-4) visualized the flow in a tubular flow reactor for supercritical hydrothermal synthesis using neutron radiography, and investigated the effects of the flow rates of two fluids and temperature of supercritical water on the mixing behavior in the reactor. In this work, the effect of reactor configuration on the mixing behavior was investigated by neutron radiography. In addition, the flow patterns and temperature distributions in the reactor were calculated using FLUENT in which the temperature and pressure dependencies of thermo-physical properties were taken into account, and were compared with the experimental results.

H. Umekawa et al. (ARS-5) have investigated the characteristics of the void fraction under several forced convective flow boiling conditions. In this report, the result under the downward flow condition was presented. The purpose of this investigation is the detailed understanding of the downward flow characteristics.

U. Matsushima et al. (ARS-6) investigated the relationship between the plant root system and water movement in a rice hull medium. It is important to know how rice hulls can be a good plant-growing medium for static solution culture without the need for aeration.

Y. Yamagata et al. (ARS-7) conducted a comparison study between neutron image taken at KUR E-2 port and RIKEN compact accelerator-driven neutron source (RANS) and X-ray CT. It was confirmed that neutron imaging has certain advantage over X-ray.

T. Numao et al. (ARS-8) evaluated the water distribution in the hardened cement paste (HPC) using neutron radiography.

M. Kanematsu et al. (ARS-9) applied neutron radiography to detect the hydraulic behavior under high temperatures to understand the spalling phenomenon of high strength concrete, focusing on the different type of materials and mix proportions, such as limestone aggregate, silica fume and fly ash which are commonly used as admixtures for high strength concrete.

H. Kagawa et al. (ARS-10) have succeeded in shooting movies of hydrazine decomposition phenomena within the catalyst bed of the mono-propellant thruster by using Neutron Radiography. The purpose of their studies is to improve the reliability of propulsion systems involved visualization, facilitating the direct observation of the physical and chemical phenomena in a thruster which is one of the most important sub-components for spacecraft.

H. Iikura et al. (ARS-11) investigated the influence of the thickness and prism pitch of brightness enhancement films (BEFs) on the brightness and spatial resolution of a neutron imaging system.

# PR4-1 Measurements of Multiphase Dynamics by Neutron Radiography

Y. Saito, D. Ito and Y. Kawabata

Research Reactor Institute, Kyoto University

**INTRODUCTION:** Temporal limit of neutron radiography depends on a neutron flux irradiated from a neutron source. High speed imaging for fast processes require short exposures in neutron radiography, which cause severe signal noise due to the statistical variation of neutron flux. Generally, time averaging can be applied to reduce such statistical noise from the original images. However, such time averaging cannot be used for motion pictures, which may cause image blurring in the filtered images. Spatial filters can be used for high frame-rate neutron radiography, however, if the S/N ratio (signal to noise ratio) is really poor, the spatial noise cannot be removed just by applying such spatial filters. Thus, it is indispensable to reduce noise from an original image by applying a temporal and spatial filter at the same time. The purpose of this study is to apply a spatio-temporal filter to high frame-rate neutron radiography to enhance quality of images and to compare the effect of neutron flux from the neutron sources.

## SPATIO-TEMPORAL FILTER:

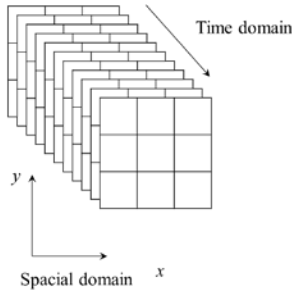


Fig. 1 Time domain and spatial domain for the modified bilateral filtering.

In general, the value of the filtered image at a given location is a function of the values of the input image in a small neighborhood of the same location. Anisotropic diffusion is a popular filtering method and the diffusion methods average over extended regions by solving partial differential equations, and is therefore inherently iterative. Iteration may raise issues of stability and, depending on the computational architecture, which are well discussed in literatures. On the other hand, Bilateral filter smooths images while preserving the edge, none iterative, local and simple. At the present study, we propose a simple modification to the original bilateral filter as follows:

$$B(s, t) = \frac{\sum_{t_p} \sum_{p \in N_s} g(\|(p, t_p) - (s, t)\|, \sigma_d) g(I(p, t_p) - I(s, t), \sigma_i) I(s, t)}{\sum_{t_p} \sum_{p \in N_s} g(\|(p, t_p) - (s, t)\|, \sigma_d) g(I(p, t_p) - I(s, t), \sigma_i)}$$

Where,  $I$  is the original gray level,  $B$  the filtered gray level, respectively.  $p(p_x, p_y)$  and  $s(s_x, s_y)$  are positions.  $t_p$  is the time domain for smoothing in the time, which was assumed to have the same weight in the spatial domain as shown in Fig.1.

## EXPERIMENTS:

The experiments were performed by using the B4-port of the Research Reactor Institute, Kyoto University. High-speed video camera (MotionPro Y4 Lite, IDT Co.Ltd.) was tested to achieve high spatial resolution (1014×1014 pixels). A high-gain, fast gated image intensifier (Single MCP (GaAsP)+Booster) by HAMAMATSU was employed to amplify the light intensity of phosphorescent images on a fluorescent converter (<sup>6</sup>LiF/ZnS:Ag). The exposure time can be adjusted by a pulse generator connected to the camera sync out. The light shielding box equipped with no optical mirror to reduce light decay and the optical axis was inclined at 45° to the neutron beam to avoid radiation damage.

**RESULTS:** The proposed spatio-temporal filtering has been applied to images obtained at the B4-port of KUR and at the JRR-3M of JAEA. Figure 1 shows the original and filtered images of two-phase mixture flowing images in a small diameter tube obtained at the B-4 port of the KUR. The exposure time was 5ms, and the successive images are shown at every 20ms. As shown in these images, it is recognized that the severe signal noises could be removed from the original images by applying the modified bilateral filter, while preserving the edge information.

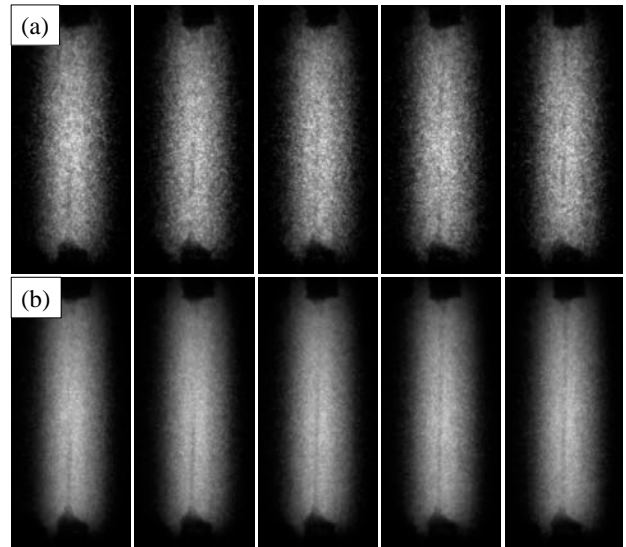


Fig.2 (a) Original two-phase flow images (b) Filtered images. ( Exposure time:5ms, tube diameter:1mm)

## PR4-2 Visualization of Two-Phase Flow in a Polymer Electrolyte Fuel Cell

N. Takenaka, H. Asano, H. Murakawa, K. Sugimoto,  
Y. Kawabata<sup>1</sup> and Y. Saito<sup>1</sup>

Graduate School of Engineering, Kobe University  
<sup>1</sup>Research Reactor Institute, Kyoto University

**INTRODUCTION:** Hydrogen combine with oxygen to form water in the cathode reaction site in a polymer electrolyte fuel cell (PEFC). The generated water may affect the fuel cell performances because of blocking the oxygen from reaching the cathode reaction site. Water management in the PEFC is important, and water distributions during the operation have been wide concern. Recently, it is reported that micro porous layer (MPL) improves the water transport in the cathode and the cell performance. However, the mechanisms have not been fully understood. Measurements of water behavior in a PEFC were carried out by using neutron radiography for understanding the water distributions in the PEFC with and without MPL.

**EXPERIMENTS:** Visualization of a PEFC were carried out with and without MPL by using neutron radiography system at B-4 port in KUR. Geometry of the PEFC was horizontal 9-parallel gas channels with equal width and depth of 1 mm. The MPL is made of carbon particle, and the thickness is about 60  $\mu\text{m}$ . The MPL is put between the gas diffusion layer (GDL) and the proton exchange membrane (PEM) at the cathode side. The GDL was TGP-H-060 (Toray Ind.) with thickness of 190  $\mu\text{m}$ , and the porosity is 0.78. The PEM was Nafion® NR-212 with thickness of 51  $\mu\text{m}$  and the area of  $10 \times 19 \text{ mm}^2$ . The images were taken by a cooled CCD camera. The exposure time was set at 60 sec. The spatial resolution which corresponds to 1 pixel was 9  $\mu\text{m}$ . Experiments were carried out at room temperature, and conditions were a current density of  $158 \text{ mA/cm}^2$ , a hydrogen flow-rate of 28 Ncc/min (utilization of 7.5%), and an air flow-rate of 66 Ncc/min (utilization of 7.5%).

**RESULTS:** Fig.1 shows two-dimensional water distributions in through-plane direction at elapse times of 6 and 12 min. The water accumulation speed in the GDL without MPL was faster than that with MPL. This tendency is remarkable at the GDL under the rib. Water evacuation from the GDL to the channel mainly occurred at the edge of the ribs. One-dimensional water distributions were calculated as shown in Fig.2. The water distributions in the GDL are completely different between without and with MPL. Water distributions takes maximum value around between the PEM and the GDL under without MPL condition. Hence, it can be confirmed that water accumulation easily occurred around catalyst layer which is located between the PEM and the GDL. On the other hand, water

accumulation smoothly distributed from the channel to the GDL, and there is no peak around the catalyst layer. These results indicate that the MPL makes change the distribution of water condensation rate in the GDL.

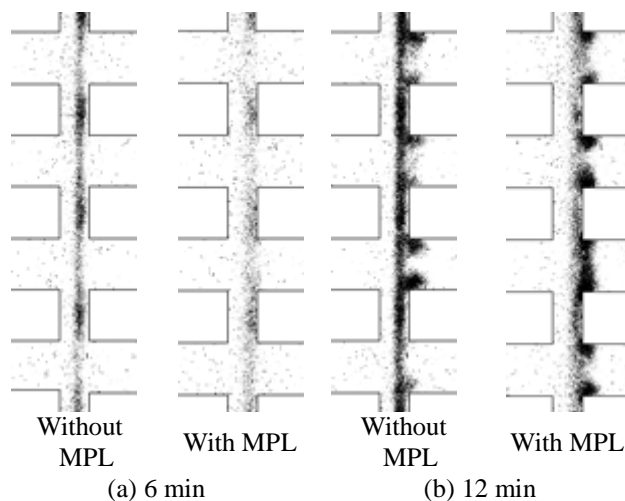


Fig. 1 Two-dimensional water distributions

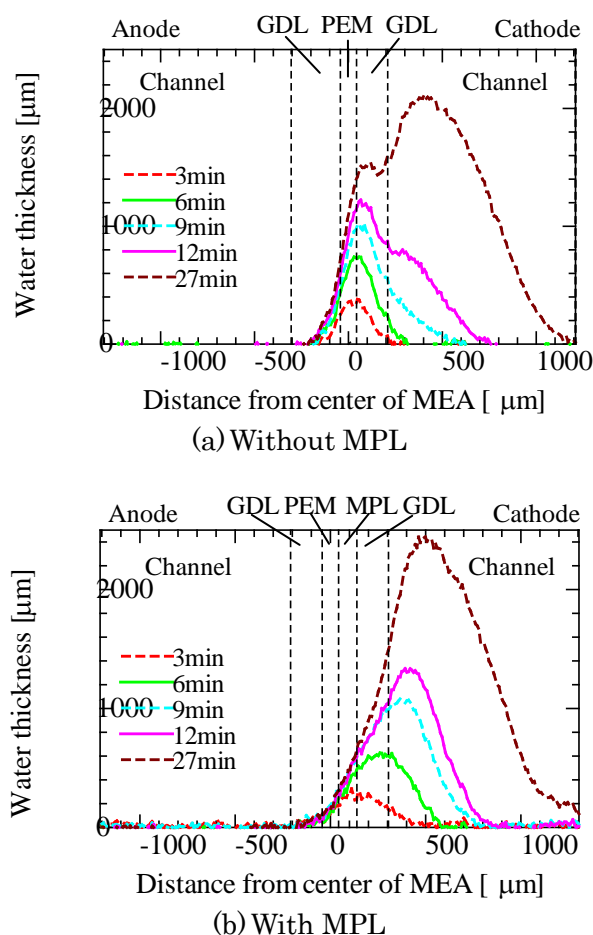


Fig. 2 Water distribution in the PEFC

## PR4-3 Neutron Radiography on Tubular Flow Reactor for Supercritical Hydrothermal Synthesis of Nanoparticles

T. Tsukada, K. Sugioka, K. Ozawa, S. Takami<sup>1</sup>,  
T. Adschiri<sup>2</sup>, K. Sugimoto<sup>3</sup>, N. Takenaka<sup>3</sup>, Y. Saito<sup>4</sup>  
and Y. Kawabata<sup>4</sup>

Dept. of Chemical Engineering, Tohoku University

<sup>1</sup>IMRAM, Tohoku University

<sup>2</sup>WPI-AIMR, Tohoku University

<sup>3</sup>Dept. of Mechanical Engineering, Kobe University

<sup>4</sup>Research Reactor Institute, Kyoto University

**INTRODUCTION:** Recently, a variety of metal-oxide nanoparticles have been synthesized by supercritical hydrothermal synthesis [1]. For the design and optimization of the process, it is important to acquire the correct knowledge about the mixing behavior of cold aqueous feed solution and supercritical water in a hydrothermal reactor. Therefore, we used neutron radiography to visualize the flow in a tubular flow reactor for supercritical hydrothermal synthesis, and investigated the effects of the flow rates of two fluids and temperature of supercritical water on the mixing behavior in the reactor [2]. In this work, the effect of reactor configuration on the mixing behavior was investigated by neutron radiography. In addition, the flow patterns and temperature distributions in the reactor were calculated using a commercial software FLUENT in which the temperature and pressure dependencies of thermophysical properties were taken into account, and were compared with the experimental results.

**EXPERIMENTS:** The tubular flow reactor has the T-junction comprised of Swagelok union tee and SUS316 tubes whose outer diameter and wall-thickness were 1/8 inch and 0.71 mm, respectively. Water at room temperature (cold water), corresponding to the feed aqueous solution, is mixed with supercritical water heated up to approximately 390°C at the T-junction. In the experiment, pressure in the reactor was set to be 25 MPa. The flow rates of supercritical water  $Q_{SC}$  were 8 and 12 g/min, and the rate of cold water  $Q_{RT}$  was varied between 1 and 6 g/min. The T-junction in the reactor, i.e., the mixing part, was irradiated by neutron beam at 1 or 5 MW power, and then the temperature distributions in the reactor were determined with the relationship between the neutron mass attenuation coefficient in water and temperature.

**RESULTS:** Fig. 1 shows the temperature distributions measured for three different reactor configurations, where  $Q_{SC} = 8.0$  g/min and  $Q_{RT} = 2.0$  g/min. The figure (a) reveals that cold water injected through the horizontal tube flows downward near the wall of the vertical tube, contacting with supercritical water at the T-junction. From the figure, it is found that a density-stratified layer is

generated by the inflow of supercritical water into the top of the horizontal tube. In the case when cold water flows downward and supercritical water is supplied into the T-junction from the side as shown in the figure (b), it can be seen that the temperature in the region above the T-junction becomes higher and uniform throughout the cross-section area of the tube. This is due to the buoyancy convection there caused by the density difference between two fluid streams. In the figure (c), the supercritical water with lower density intrudes above the room-temperature water in the left horizontal tube, and then a density-stratified layer was generated in the tube. Fig. 2 shows the numerical results of temperature distributions in the reactor corresponding to Fig.1(a), and a density-stratified layer can be observed in the horizontal tube similarly to the experimental ones.

**CONCLUSIONS:** In this work, the effect of the reactor configurations on the temperature distributions in the reactor for supercritical hydrothermal synthesis was investigated by neutron radiography, and also it was demonstrated that the numerical simulations using FLUENT can predict well the experimental results.

### REFERENCES:

- [1] T. Adschiri *et al.*, *Green Chemistry*, **13** (2011) 1380.
- [2] S. Takami *et al.*, *J. Supercrit. Fluids*, **63** (2012) 46.

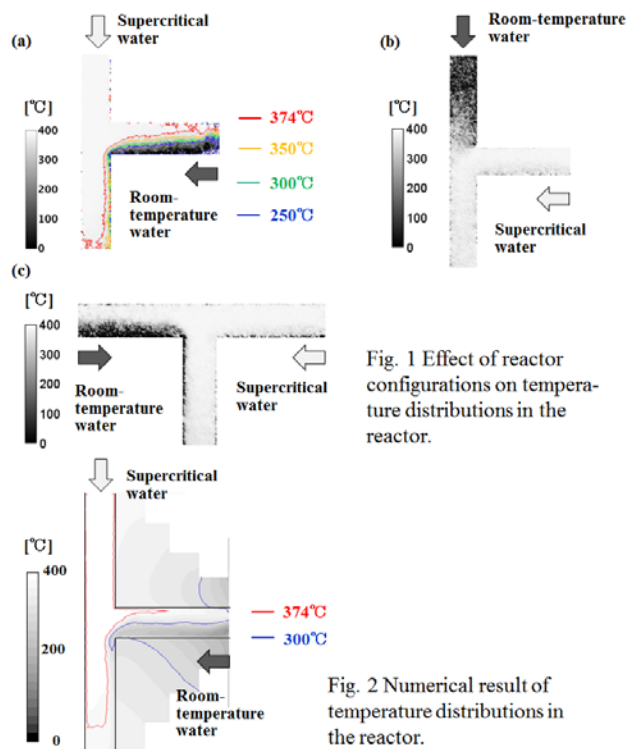


Fig. 1 Effect of reactor configurations on temperature distributions in the reactor.

Fig. 2 Numerical result of temperature distributions in the reactor.

## PR4-4 Characteristics of the Void Fraction under a Forced Convective Flow Boiling

H. Umekawa, T. Ami, K. Sakakura, S. Nakamura, S. Fujiyoshi, G. Yamashina, Y. Saito<sup>1</sup>, D. Ito<sup>1</sup> and Y. Kawabata<sup>1</sup>

Dept. Mech. Eng., Kansai University

<sup>1</sup>Research Reactor Institute, Kyoto University

**INTRODUCTION:** In this series of the project, characteristics of the void fraction under several forced convective flow boiling conditions have been estimated [1-3]. In this report, the result under the downward flow condition was presented. In the case of the downward flow, the flow direction takes the opposite direction of the buoyancy, thus several unsteady flow condition is easily occurred especially under low mass flux condition. These unsteady conditions make the understanding of the downward flow difficult. The purpose of this investigation is the detailed understanding of the downward flow characteristics.

**EXPERIMENTS:** As the visualization experiment at KUR, the void fraction of the boiling flow under upward flow and downward flow conditions have been quantitatively estimated by using thermal neutron radiography at B4 port. The working fluid was the degassed ion-exchanged water. The inner diameter of the test section was 10mm, the heated length was 400mm, and heated by using D.C. power. Besides of the visualization experiment, the measurement of the critical heat flux of several sizes of test section (I.D.= 5mm, 10mm and 15mm) was conducted at Kansai University.

In this experimental apparatus, the test section was set upon the elevating frame, and it enabled the full length visualization of the heating section even in the B4 port.

One of the thresholds of the flow characteristics of downward flow can be considered as the rising velocity of the Taylor bubble in the slug flow regime, and it can be estimated by  $0.35(gD)^{1/2}$ . This value corresponds to the  $G=95\text{kg/m}^2\text{s}$ , thus the example of the visualization results at the  $100\text{kg/m}^2\text{s}$  under upward/downward flow condition are presented in Fig.1. In the figure, the void fraction profiles along the axial direction and the radial direction at the several distances from the inlet are plotted. The location  $z$  corresponds to the distance from the inlet, and the result of the downward flow is expressed as the upside down to the actual arrangement.

These results were taken under the same conditions except flow direction, but the quite different tendency can be confirmed. Around the vapor generation point, similar void fraction profiles can be confirmed, but with the exaggerating of the boiling the difference between both flow directions become clear. For example, the drastically increasing of the void fraction of downward flow is observed at the lower quality condition compared with the upward flow. Also the premature transition from the wall peak profile along the radial direction to the center peak profile can be confirmed. These tendencies are fundamental characteristics caused by the bubble stagnation, and the understanding of these tendencies and the transition to the liquid film flow are very important to discuss the downward flow.

### REFERENCES:

- [1] H. Umekawa *et al.*, Physic. Procedia, 43(2013)269-276.
- [2] S. Nakamura *et al.*, Proc. JSME SPES2012(2012)67.
- [3] S. Fujiyoshi *et al.*, Proc. JSME SPES2012(2012)71.

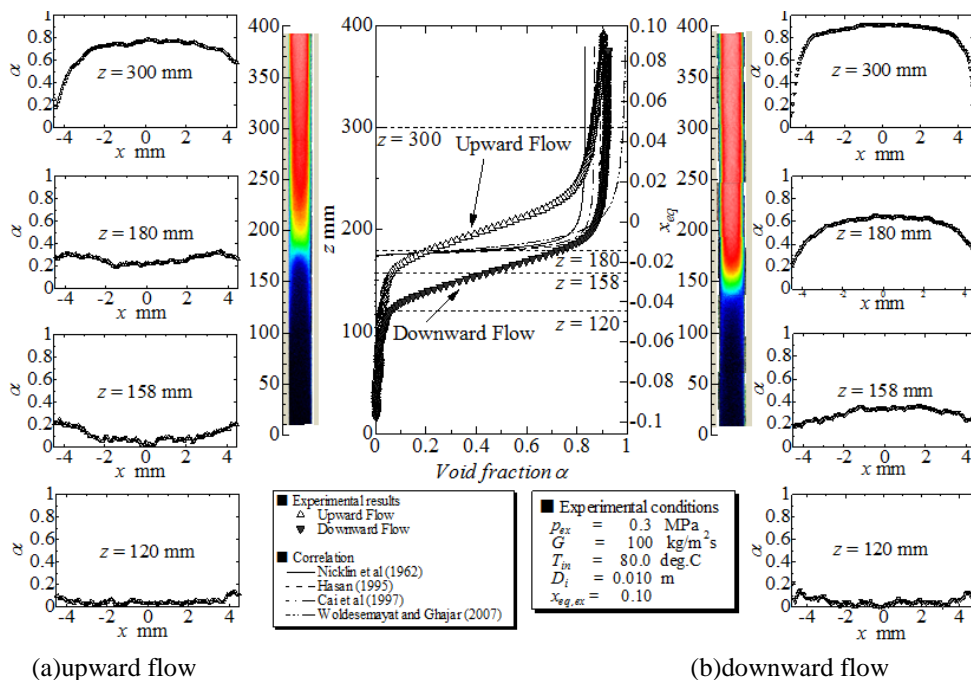


Fig.1 Comparison of void fraction profiles under upward/downward flow conditions.



## PR4-5 Relationship between Plant Root System and Water Movement in Rice Hull Medium

U. Matsushima, C. Kanno<sup>1</sup>, H. Shono and M. Okada

Faculty of Agriculture, Iwate University  
<sup>1</sup>Iwate Prefecture Government

**INTRODUCTION:** If a potted plant is placed in shallow water for an extended period, the roots will rot from remaining wet. Hence, in such watering method called “static solution culture,” it is necessary to aerate the water to provide air to the plant root; however, rice hulls can be a good plant-growing medium for static solution culture without the need for aeration. It is presumed that the large air spaces between the rice hulls make it easy for the roots to get the air they need. In addition, rice hulls do not retain water because of their structure. It is not known why the proper balance of air and water is provided in a rice hull medium. In this study, we investigated the relationship between the plant root system and water movement in a rice hull medium.

**EXPERIMENTS:** A leaf vegetable Komatsuna (*Brassica rapa* var. *perviridis* cv 'Misugi') was planted in an aluminum container (150-mm high, 50-mm wide, 20-mm deep) filled with rice hull medium. The medium contained 70% rice hulls and 30% soil. To the total volume, 3% of powdered charcoal and 5 g/L of slow-release chemical fertilizer was added. After the plant root grew and reached bottom of the container, the sample plant was placed in 50-mm-deep water for 11 days.

Neutron imaging was conducted at the E2 hole of Kyoto University Reactor (KUR). The image was captured using a CCD camera (BU-53LN, BITRAN, Saitama, Japan) with a <sup>6</sup>LiF/ZnS(Ag) scintillator. Exposure time was 5 min and 1 min for a 1 MW and 5 MW operation of KUR, respectively. The sample plant was not watered for 24 h. During this dry period, 5 neutron images were captured, after which the sample was placed in 50-mm-deep water for 24 h. During this wet period, another 5 neutron images were captured. After the images were obtained, the aluminum container was disassembled, and the plant with its developed root system was carefully removed from the rice hull medium. The bare surface of the plant was then photographed.

Image J and NI-Vision (National Instruments, Austin, Texas, USA) were used for image processing and analysis.

**RESULTS:** Figure 1-A shows the neutron image, indicating the water distribution in rice hull medium containing a root system. The degree of darkness is in proportion to the water content of the medium. Figure 1-B shows a binary image of the root system that was extracted from the photographed rice hull medium. Figure 2 shows the changes in neutron absorption by the rice hull medium in the rectangle in Fig. 1-A. The decreasing neutron absorption during the dry period indicated dehydration of the rice hull medium from transpiration by the sample plant (Fig. 2). On the contrary,

neutron absorption of the rice hull medium increased during the wet period. The increase in the water content of the medium implied by absorption was not explained by water uptake from the bottom by capillary action. It is not expected that water will reach a high level in the rice hull medium by capillary action, because the size of the rice hull particle is too big to induce long-distance water movement by capillary. In the rectangle in Figure 1-A, the root system is seen as well developed and thinner than that in the other areas (Fig. 1-B). The structure of the root system, which was expected to absorb oxygen, was often the same as that observed at the root zone in a humid atmosphere under hydroponic methods. Roots were also observed in the area that was immersed in the 50 mm of water column (Fig. 1-B). The sparse but thick root system was also observed when the roots were immersed in water. Two distinct root functions were observed in the rice hull medium: root system for respiration at the upper part and root system for the uptake of water at the bottom. However, the thin root system in the upper part required a humid habitat; therefore, the root is functioned in a manner that water is provided to the surrounding medium and a humid habitat is maintained.

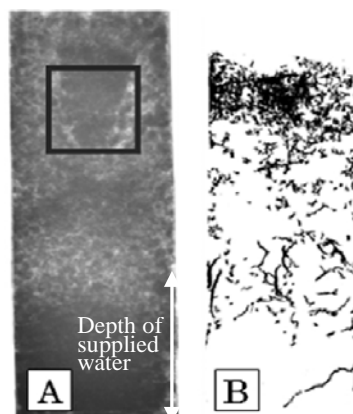


Fig.1 Water distribution in rice hull medium with a root system. A: neutron image, B: root system

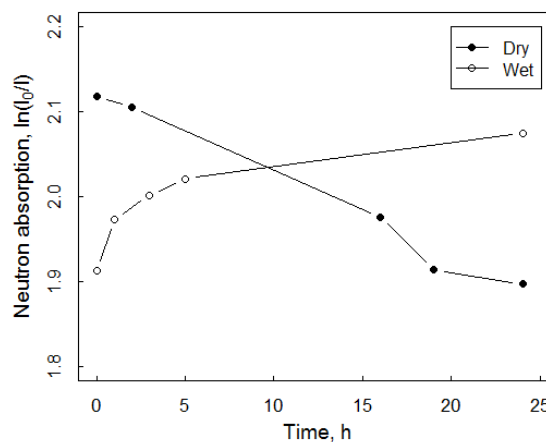


Fig.2 Changes in neutron absorption in rice hull medium

## PR4-6 Neutron Imaging of Industrial Components and Simulation Using VCAD System

Y. Yamagata<sup>1,2</sup>, K. Hirota<sup>1</sup>, S. Morita<sup>2</sup>, J. Ju<sup>2</sup>, J. Kato<sup>2</sup>,  
Y. Ohtake<sup>1,3</sup>, H. Yokota<sup>1</sup>, S. Wang<sup>1</sup>, S. Mihara<sup>2</sup>,  
H. Sunaga<sup>2</sup>, T. Sera<sup>1,4</sup>, S. Sato<sup>5</sup>, Y. Kawabata<sup>6</sup>, Y. Saito<sup>6</sup>,  
M. Hino<sup>6</sup>, M. Kitaguchi<sup>6</sup>, M. Sugiyama<sup>6</sup> and D. Ito<sup>6</sup>

<sup>1</sup>RIKEN Cluster for Innovation

<sup>2</sup>RIKEN Advanced Science Institute

<sup>3</sup>RIKEN Nishina Accelerator Research Center

<sup>4</sup>Osaka University

<sup>5</sup>KEK

<sup>6</sup>Research Reactor Institute, Kyoto University

### INTRODUCTION:

Non-destructive testing of industrial components is becoming important for recent manufacturing engineering. Neutron radiography (NR) has certain advantage over X-ray that heavy metals like steel, nickel or tungsten can be well penetrated, while light elements like hydrogen gives better contrast so that liquid inside metal structure or composite materials can be observed with better precision. However, the places where NR can be performed are limited to large institutes having research reactor or large accelerator facility. It is important to increase the chance of using neutron beams for industries for practical non-destructive testing applications related to manufacturing process.

The authors have started the construction of RIKEN compact accelerator-driven neutron source (RANS) to increase the chance of using neutron beams and it has started operation since January 2013. We conducted comparison study of NR image at KUR E-2 port and RANS. Also, comparison with x-ray CT system is carried out to illustrate the advantage of NR.

### EXPERIMENTS:



Fig. 1 A panoramic photo of RANS

Fig. 1 shows a panoramic photo of RANS. A proton linac capable of producing beam of 100 $\mu$ A on average connected to target station with beryllium target inside. Neutron beam is extracted from polyethylene moderator to the detector box at 5m distance from the target, where neutron camera with almost same configuration with that at E-2 port is situated. The neutron camera is based on a cooled CCD of 11 mega pixel with the size of 24x36mm. It has <sup>6</sup>LiF/ZnS(Ag) based scintillator with thickness of 0.1, 0.2 and 0.4mm and detection area of 150x150mm. The cooled CCD camera has 4008x2672 pixels without

binning, 2004x1336 pixels at 2x2 binning mode.

Detailed beam performance of RANS is still under inspection, but estimated thermal neutron flux at neutron camera is about 1x10<sup>4</sup>n/cm<sup>2</sup>/s with L/D of 50 at 100 $\mu$ A proton beam current.

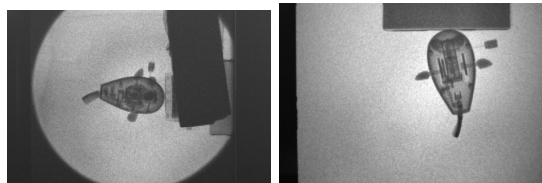


Fig2 Comparison of neutron radiography images of same bath toy taken at KUR E-2 port(left) and RANS(right) (E-2: 1MW 10sec 2x2 binning RANS: 5 $\mu$ A 5min 2x2 binning)

Fig. 2 shows neutron radiography images taken at KUR E-2 port and RANS. The quality of image at RANS is rather comparable to that of E-2 considering the beam current can be increased up to 100 $\mu$ A, neutron radiography at RANS seems to be quite practical although E-2 port is superior in L/D.

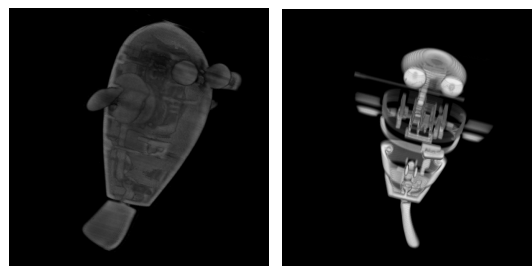


Fig.3 Comparison of CT reconstructed image by NR(E-2) and X-ray (both image was volume rendered by V-Cat using level slice)

Fig.3 shows a comparison of same bath toy CT reconstructed image by neutron radiography at E-2 port and X-ray CT scanner with 450kV x-ray tube. X-ray reconstructed image is losing some part of outer plastic shell information because there are metallic objects like gear and springs inside. Meanwhile, CT reconstructed image at E-2 shows both metallic and plastic components well. It may be possible to extract better image using more sophisticated method of region separation, but by using simple level-cut method, it was not possible.

### CONCLUSION

We have conducted a comparison study between NR image taken at KUR E-2 port and RANS and X-ray CT. It was confirmed that NR has certain advantage over X-ray. RANS will be a convenient method for NR but KUR E-2 port has still advantage in terms of beam flux and L/D.

採択課題番号 24P4-7 中性子ラジオグラフィによる工業製品の内部情報取得と プロジェクト  
VCADによるシミュレーション

(理研) 山形豊、広田克也、森田晋也、朱正明、大竹淑恵、横田秀夫、王盛、見原俊介、池上祐司、  
島崎勝輔、(大阪大) 世良俊博 (KEK) 佐藤節夫 (京大・原子炉) 川端祐司、杉山正明、齊藤泰司、  
日野正裕、北口雅暁、伊藤大介



T. Numao, N. Kumakura, Y. Matsushima, Y. Kawabata<sup>1</sup>,  
Y. Saito<sup>1</sup>, K. Watanabe<sup>2</sup>, Y. Ohno<sup>2</sup>, Y. Yamagata<sup>3</sup>, K. Hirota<sup>3</sup>  
and S. Morita<sup>3</sup>

*Department of Engineering, Ibaraki University*

<sup>1</sup>*Research Reactor Institute, Kyoto University*

<sup>2</sup>*Railway Technical Research Institute*

<sup>3</sup>*Advanced Science Center, RIKEN*

### INTRODUCTION:

In this study, two kinds of experiments were carried out to evaluate the water distribution in the hardened cement paste (HCP) using neutron radiography. One is an experiment to examine influence of the specimen thickness that the neutron transmits (Test 1). The other one is an experiment to examine the precision of the dimensions of the transmission image (Test 2).

### OUTLINE OF EXPERIMENT

#### Outline of neutron radiography examination:

Measurement of neutron radiography in this study was carried out at E2 port in KUR.

#### EXPERIMENTAL METHOD:

Figure 1 shows an Outline of Test 1. In this test, the triangular HCP specimens that thickness changes in lengthwise direction were used. This specimen was covered in aluminum foil so that water is distributed equally. Figure 3 shows the HCP specimen of the grillwork which was used for Test 2. The central length of the lattice is precisely 10mm.

#### EXPERIMENTAL RESULT AND CONSIDERATION:

Figure 2 shows an example of the result of Test 1. This result shows that neutron transmission intensity changes at thickness around 10 mm because of the extinction and dispersion of the neutron passing the water included in the specimen. The authors suggested a method to correct this result appropriately and showed that we could quantify the water content in the specimens.

Figure 4 shows an example of the result of Test 2. This result shows that the gaps between real dimensions and dimensions of the image enlarge as the distance from the center of the image becomes long. And this tendency changes by the direction from the center. It is thought that this tendency mainly depends on the optical characteristic of the CCD camera lens.

At the early drying period of the HCP, water distribution of the surface suddenly changes and influences the drying shrinkage of HCP. Therefore precision less than 1mm is required to keep the situation of the water content in HCP. The authors suggested a method to remove this influence appropriately.

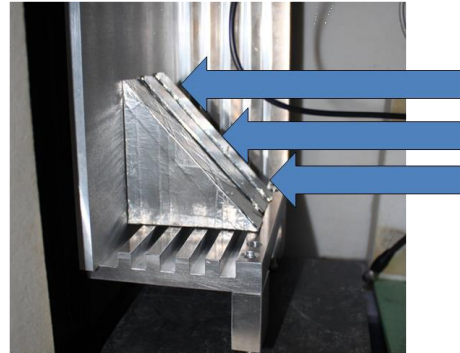


Fig.1. Outline of measurement of Test 1.

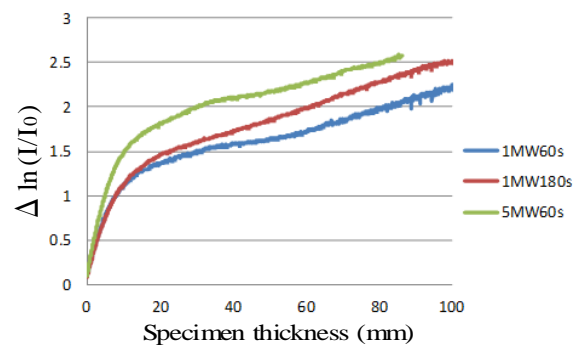


Fig. 2. Relationship between thickness and transmission intensity.

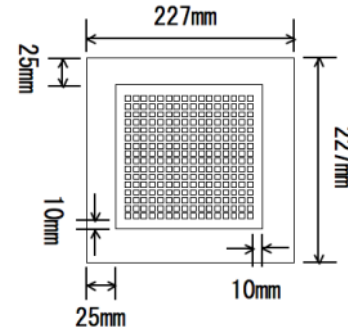


Fig 3 The specimen of Test 2.

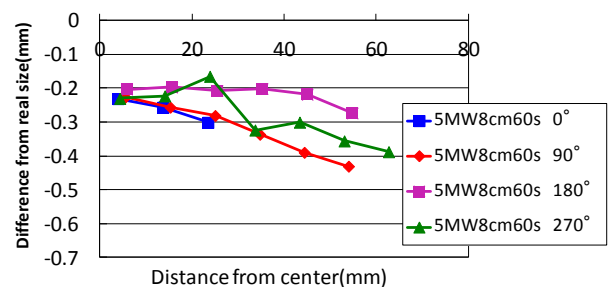


Fig.4. Difference between measurements and real size.

# PR4-8 In-situ Measurement of the Hydraulic Behavior of High Strength Concrete under High Temperature

M. Kanematsu, M. Nakano<sup>1</sup>, M. Tamura<sup>2</sup>, N. Tuchiya<sup>2</sup>, Y. Saito<sup>3</sup> and Y. Kawabata<sup>3</sup>

Faculty of Science and Technology, Tokyo University of Science

<sup>1</sup>Graduate School of Technology, Tokyo University of Science

<sup>2</sup>Graduate School of Engineering, Tokyo University

<sup>3</sup>Research Reactor Institute, Kyoto University

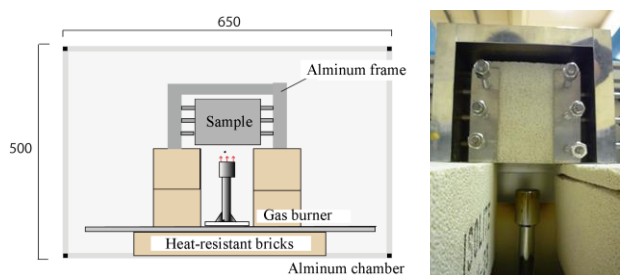


Fig. 1. Experimental setup of the heating element

**INTRODUCTION:** The exposure of reinforced concrete to unexpected high temperature may lead to spalling, fracture of the heated surface. The physicochemical process of the spalling phenomena is assumed to be due to the moisture pressure build-up inside the pore structures, restrained thermal interaction or simultaneous action of both [1]. Also, it can't be ignored that the influence of dehydrated water under high temperatures from cement hydrate, such as CSH and calcium hydrate. However the detailed mechanism of the explosive pressure formation of spalling has not been fully cleared yet.

In this research, we applied neutron radiography to detect the hydraulic behavior under high temperatures to understand the spalling phenomenon of high strength concrete, focusing on the different type of materials and mix proportions, such as limestone aggregate, silica fume and fly ash which are commonly used as admixtures for high strength concrete.

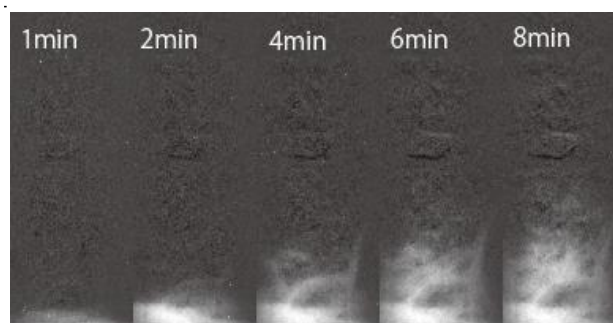
**EXPERIMENTS:** The 100x100x200 mm<sup>3</sup> prisms were used with a water cement ratio of 18% with various mix proportions. The materials that were used in this study and the mix proportion are shown in table 1. The initial water contents of the concrete samples were controlled by oven-dry under 105°C for two days. A Liquefied Petroleum (LP) gas burner was used to raise the surface temperature to 1000°C in 30 seconds and was held at 1000°C for the remainder of experiment (Fig.1).

The neutron radiography facility in the B-4 beam line of KUR was used. A neutron radiograph was obtained every 15 seconds during the heating experiment. In addition, thermal analysis by the thermogravimetry(TG) was performed to evaluate the effect of dehydrated water from cement hydrate corresponding to the temperature.

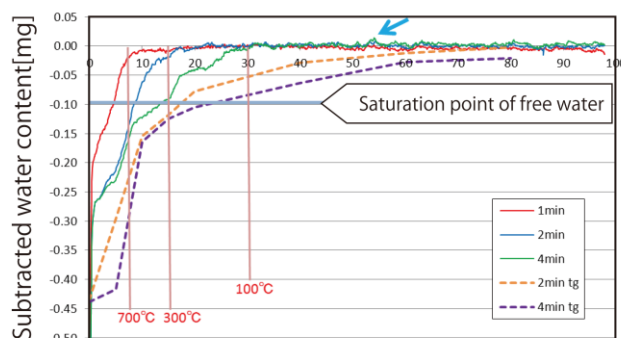
**RESULTS:** As shown in Fig. 2, the water movement of the high strength concrete (A) can be observed by the subtracted images by NRG. This result shows that between the subtracted water content observed by NRG and dehydrated moisture content calculated from the TG, differences were observed particularly in the region of 300 degrees or less. It is implied that the dehydrated water from cement hydrate remains in situ forming a high temperature and pressure.

Table 1. Mix proportions

Sample	W/B (%)	W (kg/m <sup>3</sup> )	Mass fraction			Air (%)	Materials	
			Binder (kg/m <sup>3</sup> )	Admix. replacement (%)	Sand (kg/m <sup>3</sup> )			Gravel (kg/m <sup>3</sup> )
A	18	160	888.9	10	425	1060.2	2	Silica fume
B	18	160	888.9	0	425	1060.2	2	
C	18	160	888.9	10	425	1060.2	2	Silica fume + limestone
D	18	160	888.9	10	425	1060.2	2	Fly ash



a) Subtracted images of the high strength concrete



Distance from the bottom surface(1min - 4min) [mm]

b) Comparison of subtracted water distribution with analytical value calculated from the TG

Fig. 2 The hydraulic behavior of concrete (sample A)

**REFERENCES:**

[1] F.J.Ulm, O. Coussy, Z.P.Bazant, Journal of Engineering Mechanics 125(3) (1999)272-282

## PR4-9 Hydrazine Decomposition Phenomena Observed by Neutron Radiography at a Catalyst Bed

H. Kagawa, T. Nagata, T. Masuoka, K. Kajiwara, D. Ito<sup>1</sup>, Y. Saito<sup>1</sup> and Y. Kawabata<sup>1</sup>

Propulsion Group, Japan Aerospace Exploration Agency  
<sup>1</sup>Research Reactor Institute, Kyoto University

**INTRODUCTION:** Neutron radiography can reveal invisible objects such as fluids using X-ray technology. We tried to apply this technology to observe a thruster which is one of the most important sub-components for spacecraft that uses fluids as propellants. One of our studies to improve the reliability of propulsion systems involved visualization, facilitating the direct observation of the physical and chemical phenomena occurring within the catalyst bed of the mono-propellant thruster. We have succeeded in shooting movies of hydrazine decomposition phenomena by using Neutron Radiography at Kyoto University Research Reactor.

**EXPERIMENTS:** We prepared two kinds of 1N class thruster to observe hydrazine decomposition at the catalyst bed. One had been used for JAXA's satellite propulsion system and the other is designed to extend the mission life both which were prepared by IHI Aerospace. Two thrusters were installed to the portable test equipment in parallel which was shown in Fig.1.

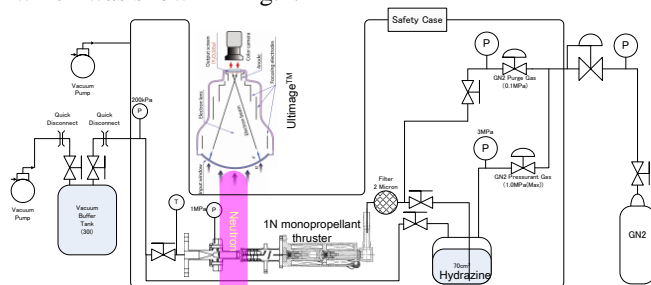


Fig. 1 The Visible Object Equipment

The observation unit was installed between the high speed observation unit and KUR B-4 imaging port, while the thrusters were operated at four feed pressure points, 2.4, 1.5, 1.0 and 0.5MPaG respectively. The imaging system is shown in Fig.2. The hydrazine injection ON time is 0.1 second, the pulse width is 0.9 second, pulse repeat number is 10. We had taken hydrazine decomposition image during hydrazine decomposition by the digital high speed camera. The image frame rate is 100 images per second.

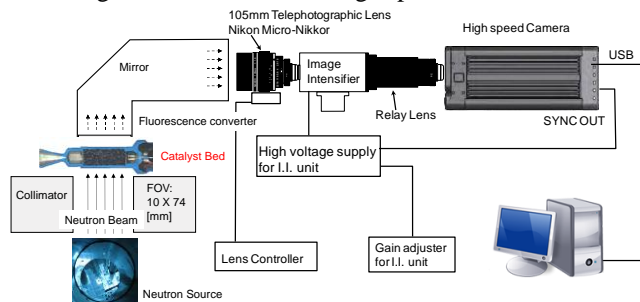
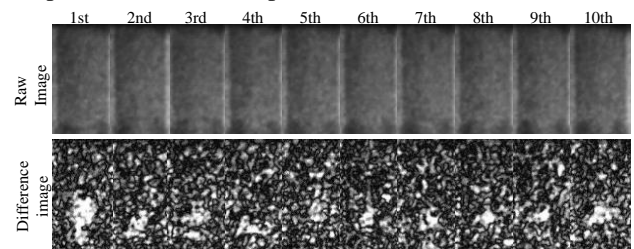


Fig. 2 The Image Acquisition System

**RESULTS:** The sample taken image of present type injector design was shown in Fig.3. The upper images were taken raw images and the lower images were processed images. Liquid hydrazine will absorb more neutrons and the raw image was made slightly dark at the hydrazine injection area. The dark area had though liquid hydrazine will present. The down row images show processed image to extend the difference before hydrazine injected and after injected. The white area part is considered liquid hydrazine has penetrated. The first pulse had wide white area.

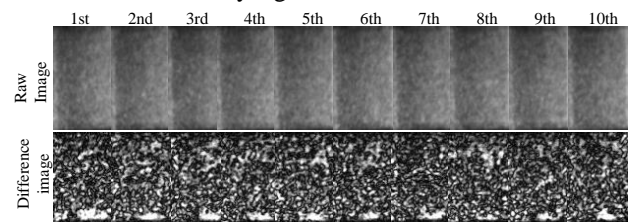
tor design was shown in Fig.3. The upper images were taken raw images and the lower images were processed images. Liquid hydrazine will absorb more neutrons and the raw image was made slightly dark at the hydrazine injection area. The dark area had though liquid hydrazine will present. The down row images show processed image to extend the difference before hydrazine injected and after injected. The white area part is considered liquid hydrazine has penetrated. The first pulse had wide white area.



0.1 sec ON / 0.9 sec OFF @ 2.4MPa G

Fig. 3 The present injector design image

The sample image of extend life type injector design was shown in Fig. 4. The injector was designed to diffusion hydrazine at the upper area of the catalyst bed. White area in the first pulse of the difference image is smaller than its penetrate type injector image. This fact shows that hydrazine penetrated widely area of catalyst bed to give soft contact to brittle catalyst granules.



0.1 sec ON / 0.9 sec OFF @ 2.4MPa G

Fig. 4 The long life injector design image

**CONCLUSIONS:** Shooting of neutrons at KUR was conducted using real hydrazine propellant and the simulated 1N thruster. The movie images showed the hydrogen liquid and hydrazine decomposition phenomena. Those images showed the hydrazine decomposition area is not depended on the injection pressure and the cold start affects the hydrazine penetrated area to wide and deep point of the 1N thruster catalyst bed. This results and technologies will be progress JAXA's longer life and high reliability thruster development activities.

### REFERENCES:

- [1] Hideshi KAGAWA and Yasushi SAITO, *et.al*, Neutron radiography used on a mono-propellant thruster, AL-AA-2011-5841, 47th Joint Propulsion Conference, 2011
- [2] Kenichi KUSHIKI, *et.al*, Visualization of propellant behavior of catalyst thruster using Neutron Radiography, B20, 49th Conference on Aerospace Propulsion and Power, 2009
- [3] Kenichi KUSHIKI, *et.al*, Visualization of Propellant Behavior inside Catalyst Thruster Using Neutron Radiography, AIAA-2009-4972, 45th Joint Propulsion Conference, 2009

H. Iikura, T. Sakai, R. Yasuda, T. Nojima,  
M. Matsubayashi, Y. Kawabata<sup>1</sup> and Y. Saito<sup>1</sup>

Quantum Beam Science Directorate, Japan Atomic Energy Agency

<sup>1</sup>Research Reactor Institute, Kyoto University

**INTRODUCTION:** We previously devised a technique for increasing the light intensity of a camera reception using brightness enhancement films (BEFs) [1]. This technique is very simple and only requires attachment of BEFs on the output surface of a scintillator for neutron imaging. In this study, the influence of the thickness and prism pitch of BEFs on the brightness and spatial resolution of a neutron imaging system were investigated using several different types of BEFs.

**EXPERIMENTS:** Neutron imaging was carried out at the neutron radiography facility (E-2 beam hole) installed in KURRI. The camera system consists of a BU-53LN cooled charge coupled device camera (BITRAN) and an 85 mm lens (Nikon Nikkor, F = 1.4) with extension rings (Nikon). In this study, a commercial type scintillator called an NR-converter (Kasei Optonix) was used as the neutron detector. Two BEFs were stacked perpendicularly and placed on the output surface of the NR-converter, and silica glass was pressed on the films in order to stick to the converter. In this study, we investigated the brightness and spatial resolution by using 4 kinds of BEFs (Table 1).

**RESULTS:** Figure 1 shows a comparison of the brightness using each BEF. The value of the brightness was obtained by subtracting the dark current from the signal counts for the camera. The exposure time was 10 min at 1 MW or 2 min at 5 MW in reactor output. By using BEFs, the brightness was increased by approximately 2.5 ~ 2.8 times in comparison with that with no BEF. The detailed spatial resolution was evaluated based on the calculation via Fourier transformation of the modulation transfer function (MTF). The MTF was obtained from the neutron transmission ratio, and 10% of the MTF was introduced from two polynomial function curves fitted to the experimental data (Fig. 2). With respect to the spatial resolution, improvement was achieved when using a BEF with a thinner polyester substrate. In this case, because the area for scattering of the visible light inside the thinner polyester substrate is reduced, the spread of the positional information about the captured neutrons should also be reduced [2].

#### REFERENCES:

- [1] H Iikura *et al.*, Nucl. Instr. and Meth., **651** (2011) 100-104.  
[2] H Iikura *et al.*, Physics Procedia, **43** (2013) 161-168.

Table 1. Configuration of the BEFs

BEF	prism pitch (μm)	thickness (μm)		prism material
		total	polyester	
BEF-1 (BEF II 90/24)	24	140	127	standard type
BEF-2 (TBEF2-T(24)n)	24	62	50	standard type
BEF-3 (TBEF2-T(19)n)	19	60	50	standard type
BEF-4 (TBEF2-GT(24))	24	65	50	high gain type

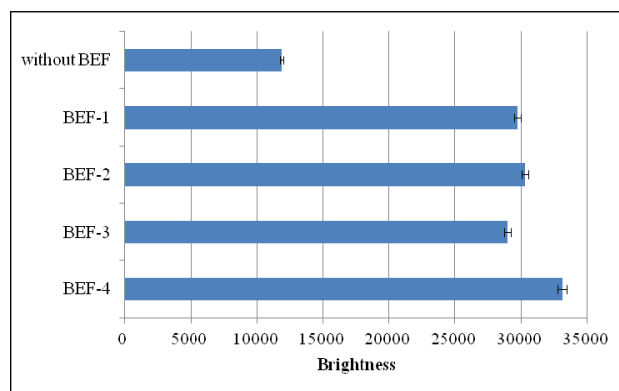


Fig. 1. Comparison of the brightness as a function of the type of BEF.

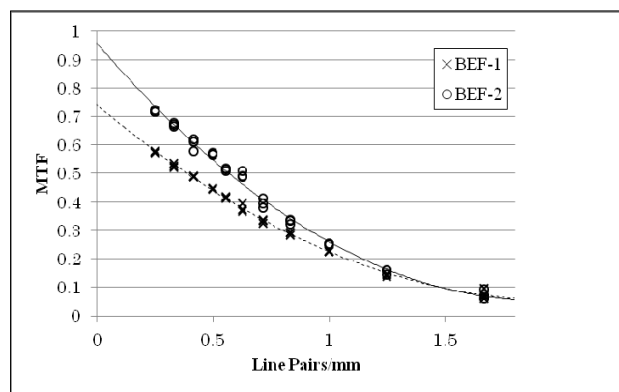


Fig. 2. MTF values using an NR-converter with BEF-1 or BEF-2. The curves were approximated using a two polynomial function to calculate each 10% MTF.